

DATASET OF INDUCED FLUORESCENCE SPECTRA FROM HUMAN LIVER BIOPSIES

JESÚS YALJÁ MONTIEL PÉREZ¹, CÉSAR CASTREJÓN PERALTA², JONATHAN AXEL CRUZ VAZQUEZ³, JOSÉ MANUEL DE LA ROSA VÁZQUEZ⁴, DIEGO ADRIAN FABILA BUSTOS⁵, KAREN ROA TORT⁶, JOSUÉ DANIEL RIVERA FERNÁNDEZ⁷, GALILEO ESCOBEDO⁸

^{1,2,3}Centro de Investigación en Computación, Instituto Politécnico Nacional, México

⁴Escuela Superior de Ingeniería Mecánica y Eléctrica-Zac, Instituto Politécnico Nacional, México

^{5,6,7}Laboratorio de optomecatrónica y energías, Unidad Profesional Interdisciplinaria de Ingeniería-Hidalgo, Instituto Politécnico Nacional, México

⁸Laboratorio de Proteómica y Metabolómica, División de Investigación, Hospital General de México, México

E-mail: ¹yalja@ipn.mx, ²castrejonp2021@cic.ipn.mx, ³jcruzv2022@cic.ipn.mx, ⁴mdelaros@ipn.mx, ⁵dfabilab@ipn.mx, ⁶kroat@ipn.mx, ⁷jdriveraf@ipn.mx, ⁸gescobedog@msn.com

ABSTRACT

Under the premise of literature identifying the molecules that constitute the liver and their alterations in disease cases, liver biopsy stages can be marked with fluorescence intensities induced by their composition. This article presents a statistical analysis of fluorescence spectra induced in 401 liver biopsies, associated with four disease states previously classified by pathologists using the METAVIR scale. The spectra are presented as a database containing 7,551 intensity measurements. To induce fluorescence in liver tissue, three light sources with wavelengths of 330 nm, 365 nm, and 405 nm were used, wavelengths close to the excitation of the main components for characterizing liver disease stages.

Keywords: *Fluorescence Spectra Of Liver, Induced Fluorescence, Medical Data Analysis, Photonics, Spectrum Dataset.*

1. INTRODUCTION

The liver is one of the largest and most complex organs in the human body. It is located in the upper right quadrant of the abdomen, just below the diaphragm. In an adult, it weighs approximately 1.4 to 1.6 kilograms. Its reddish coloration is due to its rich blood supply, and it is composed of multiple lobes.

The liver performs more than 500 essential functions for the body. It regulates the metabolism of carbohydrates, proteins, and fats. It converts glucose into glycogen (energy storage), metabolizes lipids, and produces cholesterol. It filters and removes toxins, waste products, and harmful chemicals from the blood, including alcohol, medications, and ammonia, transforming them into less toxic substances or forms that can be eliminated by the kidneys or digestive tract. The liver produces bile, a fluid essential for the digestion of fats. Bile is stored in the gallbladder and released into the small intestine when fatty foods are consumed. The liver also produces important plasma proteins such as

albumin, which maintains osmotic pressure, and clotting factors essential for wound healing and blood coagulation. It plays a role in the activation and deactivation of hormones, including the conversion of thyroxine (T4) into triiodothyronine (T3), a more active form of the thyroid hormone [1,2].

The liver is composed of various chemical substances, primarily water, which accounts for 70-75% of its weight. Water acts as a solvent for many chemical reactions and is essential for the transport of substances. The liver also consists of 15-20% proteins, including enzymes, albumin, and clotting factors, which are abundant in this organ.

Liver cells, called hepatocytes, are responsible for producing many of these proteins. The liver is also composed of 3-5% lipids, including triglycerides, cholesterol, and phospholipids, which are necessary for energy storage and the structure of cell membranes. It contains 2-8% glycogen, the stored form of glucose in the liver, which serves as a rapid energy source. The liver stores and regulates the release of fat-soluble vitamins (A, D, E, and K) and

minerals such as iron and copper, which are essential for various metabolic functions. Finally, it contains enzymes that are crucial for catalyzing biochemical reactions, such as those involved in nutrient breakdown, detoxification, and compound synthesis [3,4,5,6].

On the other hand, the liver can be affected by various diseases that compromise its ability to perform its functions. These diseases can have multiple causes, including viral infections, toxins, metabolic disorders, and autoimmune issues. Hepatitis A, B, C, D, and E are generally inflammations of the liver caused by viruses, alcohol, medications, or autoimmune diseases. Fatty liver disease (hepatic steatosis) is the excessive accumulation of fat in liver cells. Cirrhosis results from chronic liver damage that leads to scarring (fibrosis) of the liver. Healthy cells are replaced by scar tissue, severely impairing the liver's ability to function. Another liver condition is liver failure, which occurs when the liver loses its capacity to function properly, caused by factors such as viral infections, drug overdoses, or advanced cirrhosis.

Liver cancer may arise as a primary tumor or from metastasis of other organs. The most common types include hepatocellular carcinoma, the most frequent form of primary liver cancer, often associated with cirrhosis caused by hepatitis B or C, alcoholism, or fatty liver disease. The second type is cholangiocarcinoma, which affects the bile ducts both inside and outside the liver [1,7,8,9].

A diseased liver alters its normal chemical composition: there is an accumulation of triglycerides and cholesterol, a reduction in the synthesis of albumin and clotting factors, increased levels of ammonia and bilirubin, and decreased detoxification capacity. There is an imbalance of vitamins A, D, E, and K, along with the toxic accumulation of iron or copper. Excessive collagen and scar tissue are produced, glycogen storage decreases, glucose regulation is impaired, and there is a reduction in glutathione accompanied by an increase in free radicals [10,11,12,13].

The diagnosis of liver diseases involves a combination of clinical evaluations, laboratory tests, imaging studies, and, in some cases, biopsies. Physicians assess patient symptoms (such as jaundice, fatigue, weight loss, and abdominal pain) and perform physical examinations, looking for signs such as an enlarged liver or spleen (hepatomegaly, splenomegaly), fluid accumulation in the abdomen (ascites), or dilated veins on the skin (telangiectasias). The next diagnostic step includes

clinical studies aimed at detecting alterations in liver function, specifically chemical changes associated with the liver, such as elevated levels of alanine aminotransferase and aspartate aminotransferase enzymes, among others. Tests for viral hepatitis and fibrosis markers are also conducted to evaluate the degree of liver damage [7, 14,15,16,17,18].

Liver imaging tests, such as abdominal ultrasound, ultrasound elastography, computed tomography (CT), and magnetic resonance imaging (MRI), are also commonly performed. Additional tests include genetic and autoimmune screenings [14,19].

With these diagnostic methods, it is possible to accurately identify liver diseases and determine their stage or severity. However, in certain chronic cases, establishing an appropriate treatment requires a more precise assessment of inflammation levels, fibrosis severity, or the presence of accumulated substances such as iron, copper, or amyloid. A biopsy is often necessary in cases of focal liver lesions or to confirm specific conditions. This invasive and risky procedure is typically reserved for situations where it is strictly required [10,14,20,21,22,23].

Liver disease causes tissue damage, which is assessed using a scale that classifies the severity of liver fibrosis to evaluate the progression of the disease. The METAVIR scale evaluates both fibrosis (F) and inflammatory activity or necro-inflammatory grade (A). In this study, the scale is used to assess fibrosis [1,14,24]:

- F0: No fibrosis.
- F1: Portal fibrosis without septa (fibrous bridges between areas of the liver).
- F2: Portal fibrosis with a few septa.
- F3: Bridging fibrosis (advanced fibrosis), but not complete cirrhosis.
- F4: Cirrhosis (severe fibrosis affecting liver architecture).

There are other scales to assess liver damage, such as the Knodell Histological Activity Index, the Ishak scale, the Batts and Ludwig scale, the Child-Pugh scale, and the MELD scale, among others [1,14].

As mentioned, healthy liver tissue contains chemical compounds that are altered when damaged by disease. An alternative technique to assess damage as precisely as a biopsy is to evaluate the chemical or biochemical components in liver tissue

by measuring their fluorescence emission when exposed to specific lighting [25,26,27,28]. This technique is used in the present study to obtain fluorescence spectra from liver tissue samples.

The challenge lies in characterizing disease states using the METAVIR scale from liver biopsy samples. As a proposed solution, induced fluorescence is presented as a potential future alternative and non-invasive method for the liver. This technique aims to achieve greater precision in diagnosing liver disease severity, enabling the medical field to provide tailored treatments for patients. This study presents an analysis of data forming the induced fluorescence spectra, obtained experimentally by the research group at the Instituto Politécnico Nacional of Mexico, which is publicly accessible.

2. METHOD

A light source with a narrow radiation spectrum and a predominant wavelength λ , such as a laser or certain light-emitting diodes, emits photons with a specific quantum of energy associated with this wavelength [29]. The energy of a photon is given by Equation (1):

$$E = \frac{h \cdot c}{\lambda} \quad (1)$$

Where E is the energy carried by a photon, expressed in joules [J], c is the speed of light in a vacuum (3×10^8 m/s), and λ is the wavelength of the photon, expressed in meters [m].

When light with a predetermined wavelength strikes organic or inorganic material, several phenomena occur, primarily: absorption, reflection, scattering, and transmission. This interaction of light with matter is described by quantum physics. When light, which carries energy, interacts with matter, it can absorb specific wavelengths and increase its energy state. Upon releasing the absorbed energy, part of it may be emitted as heat, and part as light with lower energy than the incident light. This phenomenon is known as fluorescence and is characteristic of the molecules and atoms that make up the material [30,31].

Based on the above, an experimental setup is used to obtain the data that form the induced fluorescence spectra corresponding to the composition of liver tissue [32,33,34,35,36,37,38], as shown in Figure 1.

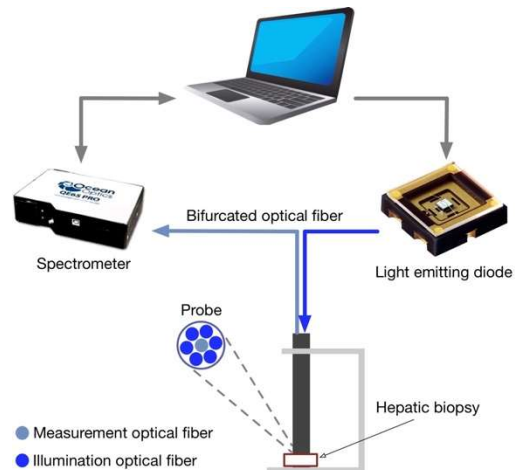


Figure 1: Experimental Setup for Spectral Data Acquisition from Human Liver Biopsies

Three light-emitting diode sources were used, emitting at wavelengths of 330 nm (UVTOP330, SETi), 365 nm (NCSU033A, Nichia), and 405 nm (405-1WUE, Violed Int.) with optical powers of 0.125, 1.25, and 0.55 mW, respectively. These wavelengths are close to those required to excite the biochemical components affected by liver disease, modifying the population of their energy levels to produce fluorescence effects [30,31,39,40].

The setup includes a bifurcated optical fiber probe (QR400-UV-VIS) and a spectrometer (QE65000-ABS) from Ocean Optics.

A computer controls the light source at a specific wavelength, which is delivered through the optical fiber to the liver biopsy, inducing fluorescence. This emitted light is captured by the optical fiber and transmitted to the spectrometer. The spectrometer performs a discrete scan over the 400–800 nm range and records intensities at each step of the scan. These data are recorded on the computer and used to generate the fluorescence spectra.

The liver tissue biopsies were provided by the Liver, Pancreas, and Motility Laboratory at the Experimental Medicine Unit, Faculty of Medicine, National Autonomous University of Mexico (UNAM)/General Hospital of Mexico "Dr. Eduardo Liceaga". The preparation of the biopsies followed a standard methodology [41] and was embedded in paraffin, with their METAVIR level already classified. The paraffin and its container exhibit fluorescence and reflection at wavelengths below

Table 1: Database.

Illumination Source	Hepatic stage	Number of spectra	Data per spectrum	Spectrum range, nm	
				min	max
330 nm	F0	29	654	400.98	899.25
	F1-F2	23	654	400.98	899.26
	F3	33	654	400.98	899.25
	F4	38	654	400.98	899.25
365 nm	F0	34	654	400.98	899.25
	F1-F2	26	654	400.98	899.26
	F3	30	654	400.98	899.25
	F4	40	654	400.98	899.26
405 nm	F0	41	580	458.96	899.25
	F1-F2	28	579	459.74	899.26
	F3	46	580	458.96	899.25
	F4	33	580	458.96	899.25

400 nm, which do not interfere with the spectral data of the tissue.

In the classification of the samples, cases of F1-F2 are grouped into a single class because even experienced pathologists are unable to distinguish between F1 and F2.

3. RESULTS

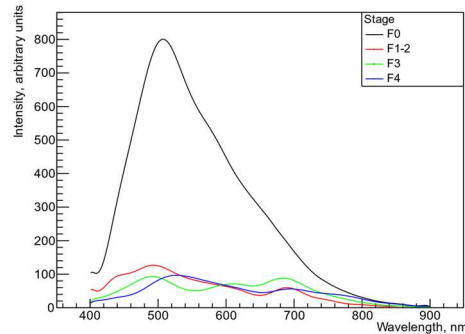
This section describes the characteristics of the dataset of induced fluorescence spectra obtained using the methodology outlined above, along with statistical characteristics and interpretations of the data.

A total of 401 spectra were recorded, corresponding to liver stages F0, F1-F2, F3, and F4, for three light sources with wavelengths of 330 nm, 365 nm, and 405 nm. The number of spectra and data per category are shown in Table 1.

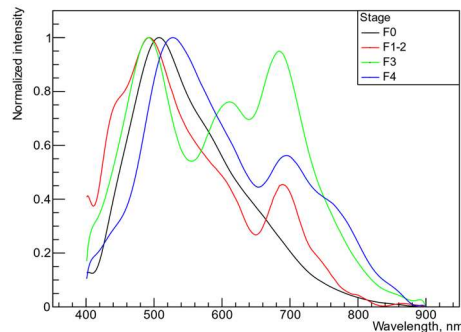
The sampling intervals obtained by the spectrometer are not uniform because, in addition to the sample, the plastic base on which the biopsy is mounted is also illuminated. This base fluoresces between 400 and 445 nm when exposed to UV light at 330 nm and 365 nm. This information does not correspond to the liver samples and has been omitted.

The spectrometer performs a discrete scan over the wavelength range with steps of 0.76 nm, recording intensities in arbitrary units per step. Luminous intensity units are not used because the spectrometer is not calibrated, providing only

relative measurement units. This aspect is reflected in the intensity values of the spectra, as shown in Figure 2-a. Therefore, it is necessary to normalize the data, as seen in Figure 2-b, where the same data are displayed in both graphs. Normalization is performed using the Equation (2).



a)



b)

Figure 2: Spectra of states F0, F1-F2, F3, and F4 irradiated at 330 nm: a) Non-normalized data, b) Normalized data.

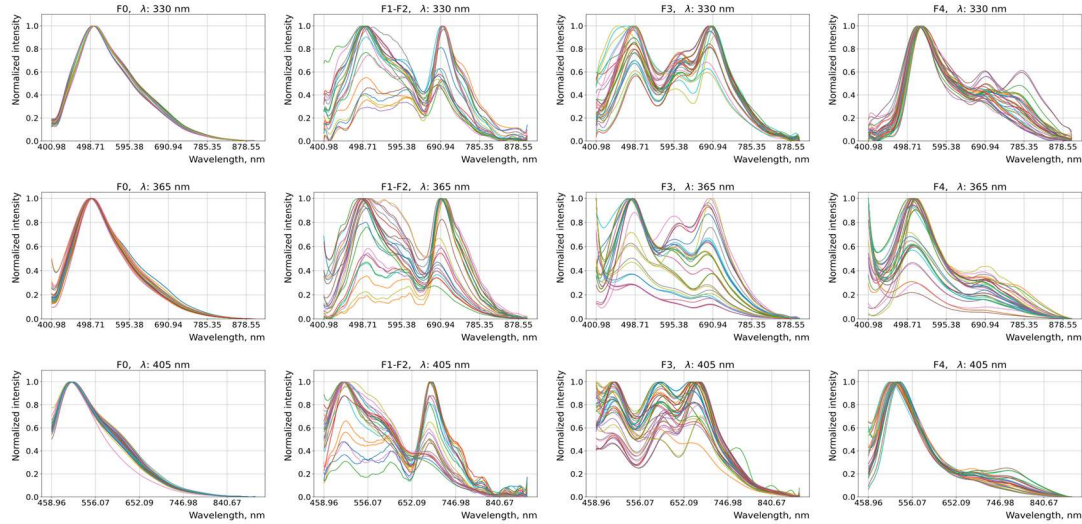


Figure 3: Normalized fluorescence spectra of liver biopsies

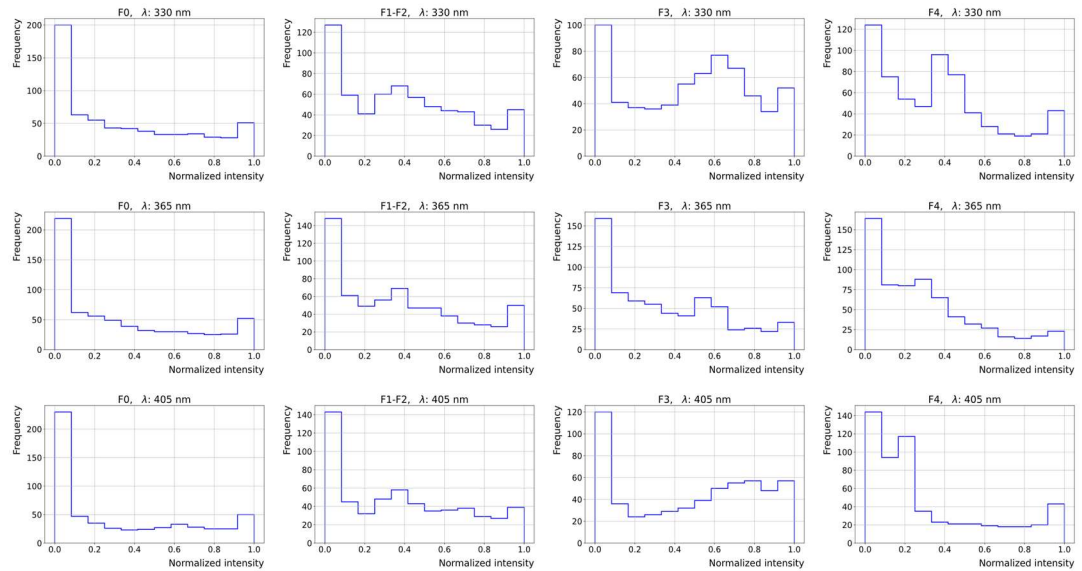


Figure 4: Average histograms of fluorescence spectra from liver biopsies

$$X_{norm} = \frac{X - \min(X)}{\max(X) - \min(X)} \quad (2)$$

Where $\min(X)$ is the minimum value and $\max(X)$ is the maximum value in a spectrum. Meanwhile, x represents the value in the spectrum to be normalized, and X_{norm} is the normalized value of X .

This calculation is performed for each data point across all spectra in the database and for the three light sources. While other processes, such as z-score normalization, which generates a distribution

with a mean of 0, could be used, normalization ensures that all records remain within the same positive value range without losing the characteristics that distinguish each stage of the disease [42].

The 401 spectra are grouped by stage and by the wavelength of the light source used. It can be observed that the healthy stage F0, across all three stage F4, which corresponds to the final stage of liver disease. For the intermediate stages F1-F2 and F3,

the spectral shape can also be characteristic but exhibits variability, as shown in Figure 3. This variability should be considered when attempting classification tasks using intelligent algorithms, as the lack of a larger database may lead to errors in the process due to the dispersion in the intermediate stages.

Figure 4 shows the average histograms for each stage by illumination wavelength. For all cases, the bin size is calculated using the Freedman-Diaconis rule, as the spectra do not exhibit any specific data distribution.

For each set of spectra, the Pearson correlation coefficient is calculated using Equation (3). This calculation is performed through permutations of the spectra, resulting in a correlation matrix for each set, as shown in Figure 5.

$$r = \frac{n \sum(XY) - \sum X \sum Y}{\sqrt{[n \sum X^2 - (\sum X)^2][n \sum Y^2 - (\sum Y)^2]}} \quad (3)$$

Where X and Y are two series for correlation, each with n data points [43].

The correlations between the spectra indicate their linear statistical relationship. In the correlation matrices graphically shown in Figure 5, correlation values close to 1 predominate, suggesting that the data follow a similar trend within each subset of spectra. That is, the spectra in a set are similar,

particularly for stages F0 and F4. In contrast, for F1-F2 and F3, the correlation suggests that the spectra within each set are not as similar. Subjectively, in Figure 3, the spectral shapes for these sets appear similar; however, the correlation factor reveals that not all spectra within the set are alike.

The similarity levels obtained with the Pearson correlation are also reflected in the standard deviation graphs shown in Figure 6. For stages F0 and F4, the data dispersion is confined within a smaller standard deviation range. In contrast, greater data dispersion is observed in the spectra corresponding to disease stages F1-F2 and F3. Specifically, the highest data dispersion is found in the F3 spectra under 365 nm illumination, followed by F4 at 365 nm and F3 at 405 nm.

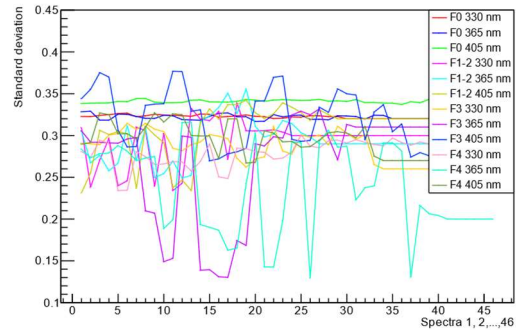


Figure 6: Standard deviation of the 401 spectra by disease level and illumination wavelength

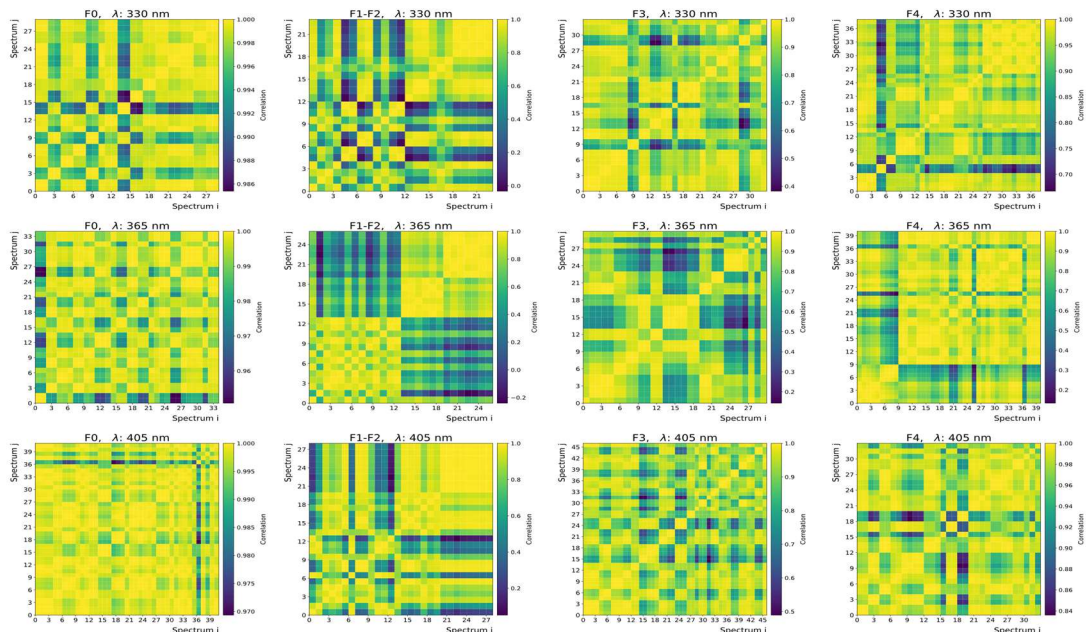


Figure 5: Correlation matrices of induced fluorescence spectra

To calculate the standard deviation of each spectrum, Equation (4) was used [44].

$$\sigma = \sqrt{\frac{1}{n} \sum_{i=0}^n (x_i - \mu)^2} \quad (4)$$

Where x_i is the i -th data point of the spectrum, n is the number of x data points in the spectrum, and σ is the standard deviation. Meanwhile, μ represents the mean of the x values, calculated using Equation (5).

$$\mu = \frac{1}{n} \sum_{i=1}^n x_i \quad (5)$$

3. CONCLUSION

Liver diseases are one of the major public health challenges worldwide. For patients to receive appropriate treatment, it is crucial to have the most accurate diagnosis possible to enhance disease management, slow its progression, and, in some cases, achieve partial recovery. The biochemistry of the molecules that make up the liver is altered by disease, producing markers detectable through fluorescence. The spectra presented differ in their intensities at specific wavelengths, which are attributed to bile salts, bilirubin, and changes in the concentrations of fat-soluble vitamins. However, no markers were identified for elastin and collagen because they were not illuminated with the wavelengths required to induce their fluorescence, as noted in the literature.

The F0 and F4 classes are clearly distinguishable through the statistical analysis presented in this work. In contrast, the statistical metrics for the F1-F2 and F3 cases are similar.

This work presents a dataset comprising induced fluorescence spectra, made available for use with artificial intelligence classifiers. The significance of this information lies in its potential to save lives through precise methods. Currently, the illumination wavelengths are 330 nm, 365 nm, and 405 nm. This leaves the door open for future work with other wavelengths, considering that light sources in this range are uncommon or not yet manufactured. In the future, the methodology described and referenced in this article could be used as a minimally invasive and laparoscopic medical tool for assessing liver damage.

ONLINE DATASET

The dataset of spectra is available at the following internet link:

<https://proyectosrym.cic.ipn.mx/#/Espectros>

If the dataset is used to generate new research, the academic institution, the authors, and this article must be cited.

ACKNOWLEDGMENTS

This work was funded by the Instituto Politécnico Nacional under the framework of the 2024 Proyectos de Desarrollo Tecnológico o Innovación, "Sistema inteligente de clasificación de estado de enfermedad en biopsias hepáticas" with SIP registration number 20242778.

We appreciate the support of the Comisión de Operación y Fomento de Actividades Académicas, COFAA-IPN; as well as the Secretaría de Ciencia, Humanidades, Tecnología e Innovación SECIHTI, México.

REFERENCES:

- [1] Arun J. Sanyal; Keith D. Lindor; Thomas D. Boyer; Norah A. Terrault; Zakim and Boyer's Hepatology: A Textbook of Liver Disease; Elsevier; 2018.
- [2] John E. Hall; Michael E. Hall; Guyton and Hall Textbook of Medical Physiology, Elsevier, 14th edition; 2021.
- [3] Patcharamon Seubnooch, Matteo Montani, Sofia Tsouka, Emmanuelle Claude, Umara Rafiqi, Aurel Perren, Jean-Francois Dufour, Mojgan Masoodi; Characterisation of hepatic lipid signature distributed across the liver zonation using mass spectrometry imaging, JHEP Reports; Volume 5, No. 6; 2023.
- [4] Sara S. Ellingwood, Alan Cheng; Biochemical and Clinical Aspects of Iycogen Storage Diseases; J Endocrinol; Vol. 238, No. 3: R131–R141; 2018.
- [5] Yongqing Hou, Shengdi Hu, Xinyu Li, Wenliang He, and Guoyao Wu; Amino Acid Metabolism in the Liver: Nutritional and Physiological Significance; Amino Acids in Nutrition and Health, Advances in Experimental Medicine and Biology 1265; Springer Nature Switzerland AG; 2020.
- [6] Jinsheng Yu, Sharon Marsh, Junbo Hu, Wenke Feng, and Chaodong Wu; The Pathogenesis of Nonalcoholic Fatty Liver Disease: Interplay between Diet, Gut Microbiota, and Genetic Background; Gastroenterology Research and Practice; 2016.
- [7] Elliot B. Tapper; Neehar D. Parikh; Diagnosis and Management of Cirrhosis and Its Complications

- A Review; Clinical Review & Education; Vol. 329, No. 18; 2023.
- [8] Rakesh Kumar Jagdish, Akash Roy, Karan Kumar, Madhumita Premkumar, Mithun Sharma, Padaki Nagaraja Rao, Duvvur Nageshwar Reddy and Anand V. Kulkarni; Pathophysiology and management of liver cirrhosis: from portal hypertension to acute-on-chronic liver failure; *Front. Med.*; 2023.
- [9] Detlef Schuppan and Nezam H. Afdhal; *Liver Cirrhosis*; *Lancet*; Vol 371; No. 9615; pp. 838-851; 2009.
- [10] James S. Dooley; Anna S. F. Lok; Guadalupe Garcia-Tsao; Massimo Pinzani; *Sherlock's Diseases of the Liver and Biliary System*; John Wiley & Sons Ltd.; 2018.
- [11] Kazuto Tajiri, Yukihiko Shimizu; Branched-chain amino acids in liver diseases; *Translational Gastroenterology and Hepatology*; Vol. 3, No. 47; 2018.
- [12] Da-Young Lee, Eun-Hee Kim; *Therapeutic Effects of Amino Acids in Liver Diseases: Current Studies and Future Perspectives*; *Journal of Cancer Prevention* Vol. 24, No. 2, 2019.
- [13] Jeongeun Hyun, Jinsol Han, Chanbin Lee, Myunghee Yoon and Youngmi Jung; *Pathophysiological Aspects of Alcohol Metabolism in the Liver*; *Int. J. Mol. Sci.* Vol. 22, No. 5717; 2021.
- [14] Lawrence Friedman, Paul Martin; *Handbook of Liver Disease*; Elsevier; 2017.
- [15] European Association for the Study of the Liver; *EASL Clinical Practice Guidelines on non-invasive tests for evaluation of liver disease severity and prognosis – 2021 update*; *Journal of Hepatology*; Vol. 75; No. 3; 2021.
- [16] Castera, L. Non-invasive assessment of liver fibrosis in chronic hepatitis C. *Hepatology* 5, 625–634; 2011.
- [17] Motola, D.L., Caravan, P., Chung, R.T. et al. Noninvasive Biomarkers of Liver Fibrosis: Clinical Applications and Future Directions. *Curr Pathobiol Rep* 2, 245–256; 2014.
- [18] Cara L. Mack, David Adams, David N. Assis, Nanda Kerkar, Michael P. Manns, Marlyn J. Mayo, John M. Vierling, Mouaz Alsawas, Mohammad H. Murad, and Albert J. Czaja; *Diagnosis and Management of Autoimmune Hepatitis in Adults and Children: 2019 Practice Guidance and Guidelines From the American Association for the Study of Liver Diseases*; *Hepatology*, Vol. 72, No. 2, 2020.
- [19] European Association for the Study of the Liver; *Clinical Practice Guidelines on the management of metabolic dysfunction-associated steatotic liver disease*; *Journal of Hepatology*, Vol. 81; pp. 492–542; September 2024.
- [20] Rockey DC, Caldwell SH, Goodman ZD, Nelson RC, Smith AD; *American Association for the Study of Liver Diseases. Liver biopsy*. *Hepatology*; Vol. 49, No. 3; pp. 1017-44; 2009.
- [21] Dominique Larrey, Lucy Meunier, José Ursic-Bedoya; *Liver Biopsy in Chronic Liver Diseases: Is There a Favorable Benefit: Risk Balance*; *Annals of Hepatology*; Vol. 16, No. 4; pp. 487-489; 2017.
- [22] Rafael Bergesch D'Incao, Marcelo Campos Appel da Silva, Paulo Roberto Lérias de Almeida, Viviane Plasse Renon, Cristiane Valle Tovo; *Percutaneous liver biopsy – 2 decades of experience in a public hospital in the South of Brazil*; *Annals of Hepatology*; Vol. 12, No. 6; pp 876-880; 2013.
- [23] Laurent Castera, Massimo Pinzani; *Biopsy and non-invasive methods for the diagnosis of liver fibrosis: does it take two to tango?*; *Gut*; Vol. 59, No. 7; pp. 861-866; 2010.
- [24] Zachary D. Goodman; *Grading and staging systems for inflammation and fibrosis in chronic liver diseases*; *Journal of Hepatology*; Vol. 47, No. 4; pp. 598-607; 2007.
- [25] Muhiudeen IA, Koerner TA, Samuelsson B, Hirabayashi Y, DeGasperi R, Li SC, Li YT. Characterization of human liver 3-O-beta-D-glucopyranuronosyl-cholesterol by mass spectrometry and nuclear magnetic resonance spectroscopy. *J Lipid Res.* Vol. 25, No. 10; 1984.
- [26] Saitou T, Takanezawa S, Ninomiya H, Watanabe T, Yamamoto S, Hiasa Y and Imamura T (2018) *Tissue Intrinsic Fluorescence Spectra-Based Digital Pathology of Liver Fibrosis by Marker-Controlled Segmentation*. *Front. Med.*; Vol.5 p. 350; 2018.
- [27] Nazeer SS, Sreedevi TP, Jayasree RS. *Autofluorescence spectroscopy and multivariate analysis for predicting the induced damages to other organs due to liver fibrosis*. *Spectrochim Acta A Mol Biomol Spectrosc.* 2021.
- [28] Amani, M., Bavali, A.; Parvin, P. *Optical characterization of the liver tissue affected by fibrolamellar hepatocellular carcinoma based on internal filters of laser-induced fluorescence*. *Sci Rep* 12, 6116; 2022.

- [29] Planck, M., Ueber das Gesetz der Energieverteilung im Normalspectrum. *Ann. Phys.*, 309: 553-563; 1901.
- [30] Joseph R. Lakowicz; *Principles of Fluorescence Spectroscopy*; Springer Science+Business Media, LLC; 2010.
- [31] Leonard Shapiro; *Microscopy Techniques for Biomedical Education and Healthcare Practice*; Springer Nature Switzerland AG; 2023.
- [32] D. Fabila, L. Hernández, J. de la Rosa, S. Stolik, U. Arroyo-Camarena, M. López-Vancell y G. Escobedo, «Optical spectroscopy for differentiation of liver tissue under distinct stages of fibrosis: an ex vivo study» 8th Iberoamerican Optics Meeting and 11th Latin American Meeting on Optics, Laser and Applications, Portugal, 2013
- [33] D. A. Fabila Bustos, U. D. Arroyo Camarena, M. D. López Vancell, M. A. Durán Padilla, I. Azuceno García, S. Stolik Isakina, E. Ibarra Coronado, B. Brown, G. Escobedo y J. M. de la Rosa Vázquez, «Diffuse Reflectance Spectroscopy as a Possible Tool to Complement Liver Biopsy for Grading Hepatic Fibrosis in Paraffin-Preserved Human Liver Specimens» *Applied Spectroscopy*, vol. 68, no 12, pp. 1357-1364, 2014.
- [34] D. A. Fabila Bustos, *Estudio de la Fluorescencia y Reflectancia Difusa en Tejido Biológico (Fibrosis Hepática-Cáncer)*, Tesis para obtener el título de Doctor en Comunicaciones y Electrónica, IPN, 2014.
- [35] D. A. Fabila-Bustos, Ú. D. Arroyo-Camarena, M. D. López-Vancell, M. A. Durán-Padilla, I. Azuceno-García, S. Stolik-Isakina, A. Valor-Reed, E. Ibarra-Coronado, L. F. Hernández-Quintanar, G. Escobedo y J. M. de la Rosa-Vázquez, «Fluorescence Spectroscopy as a Tool for the Assessment Liver Samples with Several Stages of Fibrosis,» *Photomedicine and laser surgery*, vol. 36, no 3, pp. 151-161, 2018.
- [36] Eduardo J. Arista Romeu, Josué D. Rivera Fernández, Karen Roa Tort, Alma Valor, Galileo Escobedo, Diego A. Fabila Bustos, Suren Stolik, José Manuel de la Rosa, Carolina Guzmán; *Combined methods of optical spectroscopy and artificial intelligence in the assessment of experimentally induced non-alcoholic fatty liver*; *Computer Methods and Programs in Biomedicine*; Volume 198, 2021.
- [37] Karen Roa-Tort, Josué D. Rivera-Fernández, José M. de la Rosa-Vázquez, Galileo Escobedo, Suren Stolik, Alma Valor, Diego A. Fabila-Bustos, *Fluorescence spectroscopy on paraffin-preserved human liver samples to classify several grades of fibrosis*, *Spectrochimica Acta Part A: Molecular and Biomolecular Spectroscopy*, Volume 242, 2020.
- [38] Karen Roa-Tort; *Análisis y clasificación de biopsias incluidas en parafina a través de métodos espectroscópicos*; Tesis para obtener el título de Doctor en Comunicaciones y Electrónica, IPN, 2020.
- [39] N. Ramanujam, *Fluorescence Spectroscopy in Vivo*, *Encyclopedia of Analytical Chemistry*, 2011.
- [40] M. da Silva Baptista y E. Leite Bastos, «Fluorescence in Pharmaceutics and Cosmetics» *de Fluorescence in Industry*, Lisboa, Springer, 2019.
- [41] F. Brenes-Pino, «Histología de la biopsia hepática, enfoque clínico,» *Acta Médica Costarricense*, vol. 50, no 3, pp. 17-20, 2008.
- [42] Cabello-Solorzano, K., Ortigosa de Araujo, I., Peña, M., Correia, L., J. Tallón-Ballesteros, A. (2023). The Impact of Data Normalization on the Accuracy of Machine Learning Algorithms: A Comparative Analysis. In: García Bringas, P., et al. 18th International Conference on Soft Computing Models in Industrial and Environmental Applications (SOCO 2023). SOCO 2023. *Lecture Notes in Networks and Systems*, vol 750. Springer, 2023.
- [43] Joseph Lee Rodgers; W. Alan Nicewander; *Thirteen Ways to Look at the Correlation Coefficient*; *The American Statistician*, Vol. 42, No. 1.; 1988.
- [44] Pham, Hoang; *Springer Handbook of Engineering Statistics*, Springer Nature; 2023.